

Photon-correlation Fourier spectroscopy of the trion fluorescence in thick-shell CdSe/CdS nanocrystals

L Biadala, H Frederich, L Coolen, S Buil, X Quélin, C Javaux, M Nasilowski,
B Dubertret, J.-P Hermier

► **To cite this version:**

L Biadala, H Frederich, L Coolen, S Buil, X Quélin, et al.. Photon-correlation Fourier spectroscopy of the trion fluorescence in thick-shell CdSe/CdS nanocrystals. *Physical Review B : Condensed matter and materials physics*, American Physical Society, 2015, 91 (8), pp.085416. <10.1103/PhysRevB.91.085416>. <hal-01337654>

HAL Id: hal-01337654

<https://hal-uvsq.archives-ouvertes.fr/hal-01337654>

Submitted on 27 Jun 2016

HAL is a multi-disciplinary open access archive for the deposit and dissemination of scientific research documents, whether they are published or not. The documents may come from teaching and research institutions in France or abroad, or from public or private research centers.

L'archive ouverte pluridisciplinaire **HAL**, est destinée au dépôt et à la diffusion de documents scientifiques de niveau recherche, publiés ou non, émanant des établissements d'enseignement et de recherche français ou étrangers, des laboratoires publics ou privés.

Photon-correlation Fourier spectroscopy of the trion fluorescence in thick-shell CdSe/CdS nanocrystals

L. Biadala,¹ H. Frederich,¹ L. Coolen,^{2,3} S. Buil,¹ X. Quélin,¹ C. Javaux,⁴ M. Nasilowski,⁴
B. Dubertret,⁴ and J.-P. Hermier^{1,5,*}

¹*Groupe d'Étude de la Matière Condensée, Université de Versailles-Saint-Quentin-en-Yvelines, CNRS UMR 8635, 45, Avenue des États-Unis, F-78035 Versailles, France*

²*Sorbonne Universités, UPMC Univ Paris 06, UMR 7588, Institut de NanoSciences de Paris (INSP), F-75005 Paris, France*

³*CNRS UMR 7588, Institut de NanoSciences de Paris (INSP), F-75005 Paris, France*

⁴*Laboratoire de Physique et d'Étude des Matériaux, CNRS UMR 8213, ESPCI, 10, Rue Vauquelin, F-75231 Paris, France*

⁵*Institut Universitaire de France, 103, Boulevard Saint-Michel, F-75005 Paris, France*

(Received 13 June 2014; revised manuscript received 7 November 2014; published 18 February 2015)

The emission spectrum of the trion state in very thick shell CdSe/CdS nanocrystals is characterized at 4 K by photon correlation Fourier spectroscopy. A value of 50 μeV for the width of the zero phonon line is measured. The absence of blinking and the high photostability of these emitters offer the possibility to investigate the dynamics of the emission spectrum at a time scale as short as 250 ns. We show that the high value of the linewidth (50 μeV) is not due to spectral diffusion induced by the close environment of the emitter at time scales larger than 250 ns. The broadening is attributed to the additional third carrier when compared to the monoexcitonic state.

DOI: [10.1103/PhysRevB.91.085416](https://doi.org/10.1103/PhysRevB.91.085416)

PACS number(s): 78.47.-p, 42.50.Ar, 73.63.Bd

I. INTRODUCTION

The growth of a crystalline CdS thick shell on a CdSe core has been a crucial improvement for semiconductor nanocrystals (NCs) [1,2]. Compared to previous standard CdSe/ZnS NCs, blinking is greatly reduced. Off periods longer than 100 ms are no longer observed and, even if flickering still occurs, complete extinction is never reached. This last property results from the low rate of nonradiative Auger recombinations when the NC is ionized [3–5].

It was established that these specific NCs are negatively charged at 4 K and that the Auger processes for the negative trion state (two electrons and one hole) are thermally activated [6]. At room temperature, one of the two electrons is delocalized in the whole core-shell structure. It probes the abrupt potential step at the NC surface, that enhances nonradiative Auger recombination. At cryogenic temperatures, the three carriers get confined in the core and Auger process is completely inhibited. As a result, the radiative quantum yield (QY) of the negative trion state is close to 1 under 30 K and perfectly stable at time scales ranging from 50 ns to 100 ms [7]. The negative trion state then appears as a perfect emitting state for which the two electrons and the hole are localized only in the core of the NC and isolated from the environment by the thick CdS shell.

From a general point of view, the interaction between a NC and its close environment is at the very origin of flickering [8]. In addition to blinking, this interaction leads to the well-known phenomenon of spectral diffusion (SD) that can be revealed by single emitter microscopy [9,10]. Trapping and movements of charges at the shell-ligands interface result in fluctuations of the local electric field that induce random spectral jumps and broaden the emission linewidth. The dynamics of the SD has received great interest [11–14] since it limits the use of colloidal NC in applications such as two-photon interference

in the domain of quantum computing for which time coherence is a key point. SD can be studied using either conventional spectroscopic technique, which is based on the acquisition of consecutive photoluminescence (PL) spectra [13], or by more advanced methods. Due to practical limitations linked to the collection efficiency of the experimental setup, high resolution spectroscopic techniques have to be used on faster time scales than few ms. Plakhotnik *et al.* were the pioneers of fast spectroscopic techniques [15]. From 1998, other experimental techniques were developed. Sallen *et al.* showed that subnanosecond spectral diffusion can be measured through the correlations of photons emitted within two spectral windows that are narrower than the SD broadened line [16]. Two other techniques, correlation interferometry and photon correlation Fourier spectroscopy (PCFS), are based on the time correlations of the photons detected at the two outputs of a Michelson interferometer [17–21]. Taking advantage of the high spectral resolution of an interferometer, PCFS provides a lower temporal resolution but a more accurate analysis in terms of SD amplitude. Combined with fluorescence correlation spectroscopy (FCS), PCFS also enables to extract single fluorophore linewidth from a solution of NCs [22].

Recently, results on the SD dynamics for 5-nm shell CdSe/CdS NCs were reported [23]. Combining PCFS and standard single-emitter spectroscopy, Beyler *et al.* showed that the SD is characterized by rapid discrete spectral jumps at short time scales (≤ 10 ms) and quasicontinuous diffusion at longer time scales. For this shell thickness, charging and neutralization of the NC still occurs and induces spectral jumps of about 20 meV. Intensity fluctuations are observed and the QY of the trion and monoexcitonic states are not equal. Moreover, even if a single mechanism can describe the SD dynamics, its parameters depend dramatically on the NC showing the crucial influence of the QD surface.

In this paper, the PCFS method is applied to CdSe/CdS NCs with a shell thicker than 10 nm that is always negatively photocharged at 4 K. First, a standard spectroscopic measurement allows us to identify the respective contributions

*jean-pierre.hermier@uvsq.fr

of the zero phonon line (ZPL), its acoustic phonon sideband, and the phonon longitudinal-optical replicas. PCFS is then used to measure the linewidth for the ZPL. A value of $50 \mu\text{eV}$ is reported. Since no blinking is observed, the intensity fluctuations follow a Poisson distribution, which opens the possibility for the PCFS method to investigate the effect of SD on the emission linewidth at time scales as short as 250 ns. We show that the effect of the SD due to the NC surrounding environment is low on a time scale ranging between 250 ns and 10 ms. We attribute the large measured linewidth of the trion state to the presence of a third charge in comparison to the exciton. The additional charge increases the polarizability of the emitting state and makes it more sensitive to very fast electrical local field fluctuations. Very fast SD may be then at the origin of the measured linewidth broadening.

II. EXPERIMENT

A. Experimental setup

CdSe/CdS core-shell NCs used in this study were synthesized by the authors [1]. They have a 3-nm core radius and a thick shell of 11 nm (± 1 nm). At room temperature, the ensemble photoluminescence (PL) spectrum shows that they emit around 660 nm (full width at half maximum of 32 nm). At 4K, the PL spectrum is centered at 630 nm (1.97 eV). The NCs are deposited on a sapphire coverslip with a spin coater so that they can be observed at the single molecule level with a confocal microscope (IX 71, Olympus). The sample is placed in a cryostat with a continuous flow of helium (Microstat-He HiRes, Oxford Instruments). The NCs are optically excited far from resonance with a continuous wave laser diode (LDH-P-C 405, Picoquant, wavelength ~ 405 nm). Weak excitation was used to prevent biexcitonic emission. The fluorescence is collected by an objective with a 0.7 numerical aperture and characterized by a spectrometer (600 or 1800 grooves/mm, focal length 75 cm) or a Michelson interferometer that consists in a nonpolarizing beam splitter and two retroreflectors. A 20 cm translation stage enables to move one of the retroreflector with a constant speed equal to $1 \mu\text{m/s}$. The position of this retroreflector is also controlled with a piezoelectric actuator (scan range of $15 \mu\text{m}$).

Two avalanche photodiodes (SPCM-AQR-13, Perkin-Elmer) are placed at the outputs of the Michelson. They are connected to a PicoHarp 300 module (Picoquant) that provides the absolute time for each detection event with a precision equal to the time resolution of the photodiodes (300 ps). A single data set gives the variation of the fluorescence intensity with time and the histogram of the delays between photons at the outputs of the interferometer [24].

B. Data analysis

The recorded data will be analyzed following the PCFS method. From a general point of view, standard Fourier spectroscopy is a well-known technique that provides the spectrum of a radiative source making the Fourier transform of the contrast of the interference fringes measured at the output of a scanning interferometer. However, when spectral diffusion occurs at a time scale shorter than the time bin used to measure the fringes contrast, standard Fourier spectroscopy

is irrelevant. The photon correlation Fourier spectroscopy method overcomes this limitation. It relies on the fact that spectral fluctuations can be directly encoded in the correlation functions $G_{ij}(t, \tau) = \overline{I_i(t)I_j(t + \tau)}$ (i and $j = a$ or b) of the intensities detected by the photodiodes (noted a and b) placed at the outputs of the Michelson interferometer. The correlations can then be used to get the contrast $\mathcal{C}(d_t)$ for a temporal path difference d_t . In the following, the lowest value of $\delta\tau$ (the time resolution on τ) will be equal to 250 ns [17,18].

The contrast can be calculated through the following normalized function [19]:

$$G_n(t, \tau) = \frac{\sqrt{\tilde{G}_{aa}\tilde{G}_{bb}} - (\tilde{G}_{ba} + \tilde{G}_{ab})/2}{\sqrt{\tilde{G}_{aa}\tilde{G}_{bb}} + (\tilde{G}_{ba} + \tilde{G}_{ab})/2}(t, \tau), \quad (1)$$

where $\tilde{G}_{ij}(t, \tau)$ takes into account the background signals as defined in Ref. [19].

Because it considers all the autocorrelation functions [$\overline{I_a(t)I_a(t + \tau)}$, $\overline{I_b(t)I_b(t + \tau)}$ and $\overline{I_a(t)I_b(t + \tau)}$] that can be measured, such an approach improves the accuracy of the result. The role of the normalized function is also, for flickering emitters such as standard CdSe/ZnS nanocrystals, to correct for the fluctuations of the total emitted intensity. However, at short time scales ($\tau \leq 2 \mu\text{s}$), after-pulsing in avalanche photodiodes distorts the value of $\overline{I_a(t)I_a(t + \tau)}$ and $\overline{I_b(t)I_b(t + \tau)}$ and prevents the correct calculation of $G_n(t, \tau)$. For such short delays, only cross-correlations terms $\overline{I_a(t)I_b(t + \tau)}$ and $\overline{I_b(t)I_a(t + \tau)}$ can be measured correctly and provide information (see Sec. III C).

III. FLUORESCENCE PROPERTIES OF SINGLE CDSE/CDS NCS AT 4K

A. Standard spectroscopy

At 4 K, a NC with such a thick shell remains always ionized [6]. Auger recombinations are suppressed and the trion state recombines radiatively with a lifetime of the order of 6 ns [see inset Fig. 1(a)]. The PL spectrum of the same NC (noted NC₁) recorded with a 600 grooves/mm grating under continuous excitation displays a sharp zero phonon line (ZPL), taken as the reference of the energies, an optical (LO) phonon replica and a longitudinal acoustic (LA) pedestal [Fig. 1(a)]. Interestingly LO phonon from CdSe and CdS, red shifted from the ZPL by 26.7 meV and 36 meV, respectively, are clearly observed. It is noteworthy that the weakness of the CdS phonon replica confirms that the two electrons of the trion are confined in the CdSe core [25], i.e., the charge carriers are far from the CdS shell/ligand interface. In the following, we will see that the NC surface plays little role in the broadening of the ZPL linewidth. Figure 1(b) displays a high resolution spectrum (1800 grooves/mm grating) of the same NC around the main excitonic peak. Besides a broadened LA phonon sideband, the PL spectrum shows a resolution-limited ZPL linewidth of $150 \mu\text{eV}$.

B. Photon correlation Fourier spectroscopy methodology

The PCFS analysis is now presented. The lowest value of the time resolution on the delay between photons ($\delta\tau = 250$ ns) is much greater than the radiative lifetime and a quantum formalism is not needed [17]. The correlation functions

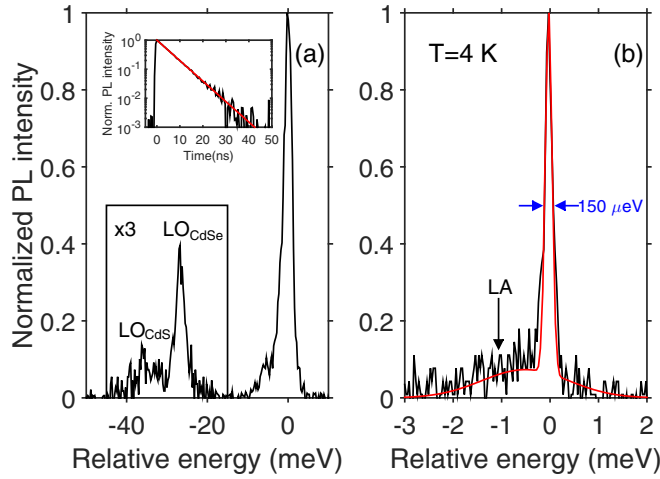


FIG. 1. (Color online) (a) PL spectrum of a single NC at 4 K (acquisition time of 10 s, 600 grooves/mm grating). The zero phonon line (ZPL), the respective contributions of the CdSe and CdS (LO) phonon replica are indicated. For clarity, the LO phonon sideband is enhanced by a factor 3. Inset: photoluminescence decay of the fluorescence intensity. The red line is a monoexponential decay corresponding to a lifetime of 6 ns. (b) PL spectrum with a 1800 grooves/mm grating (acquisition time of 1 s) showing a sharp ZPL together with a broadened acoustic phonon tail. The red line is a fit with two Gaussians having a full width at half maximum (FWHM) of 150 μeV and 1.8 meV. Note that the reference of the energy is 1.9211 eV.

$\tilde{G}_{ij}(t, \tau)$ then write

$$\tilde{G}_{ij}(t, \tau) = \frac{I(t)I(t + \tau)}{4} \left\{ 1 + \frac{\varepsilon_i \varepsilon_j}{2} \mathcal{C}^2(d_t) \hat{p}_\tau(d_t) \times \cos[\omega_0(d_t - d_{t+\tau})] \right\}, \quad (2)$$

where $\varepsilon_a = 1$, $\varepsilon_b = -1$. $\hat{p}_\tau(d_t)$ is the Fourier transform of the statistic of the spectral jumps $p_\tau(\zeta)$ during τ [$p_\tau(\zeta)$ is the probability that the frequency shift between times t and $t + \tau$ is equal to ζ] [17].

The normalized function $G_n(t, \tau)$ defined by Eq. (1) is

$$G_n(t, \tau) = \frac{1}{2} \mathcal{C}^2(d_t) \hat{p}_\tau(d_t) \cos[\omega_0(d_t - d_{t+\tau})]. \quad (3)$$

For $\tau < 1$ ms and a speed of the translation stage equal to 1 $\mu\text{m/s}$, $\cos[\omega_0(d_t - d_{t+\tau})] \sim 1$ and

$$G_n(t, \tau) = \frac{1}{2} \mathcal{C}^2(d_t) \hat{p}_\tau(d_t). \quad (4)$$

$\sqrt{2G_n(t, \tau)}$ then corresponds to the value of the contrast for given path delay d_t mitigated by the term $\sqrt{\hat{p}_\tau(d_t)}$ so $\mathcal{C}(d_t) = \sqrt{2G_n(t, \tau \rightarrow 0)}$. The Fourier transform of $\sqrt{2G_n(t, \tau)}$ (as a function of d_t) appears as the PL spectrum broadened by the SD during τ . A better spectral resolution is thus achieved when a shorter τ value is considered. We must stress that the time resolution $\delta\tau$ on τ of the experiment is only limited by the number of photons pairs detected during $\delta\tau$. In contrast with conventional spectroscopic techniques, the resolution of PCFS increases with the integration time since more and more photon pairs are detected. In the following, we start with ms values of τ , which is sufficient to analyze the spectrum phonon

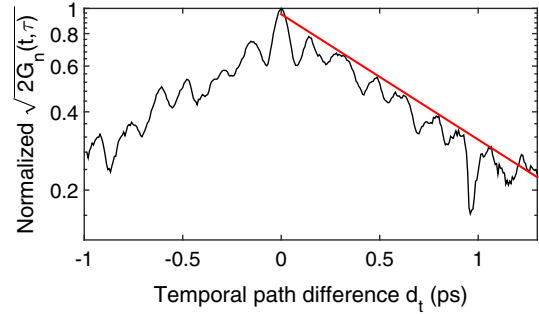


FIG. 2. (Color online) Normalized value of $\sqrt{2G_n(t, \tau)}$ measured by PCFS for $\tau = 1$ ms as a function of the time path difference (in semilog scale). The normalization is made with the value of $\sqrt{2G_n(t, \tau)}$ at zero delay. The red line corresponds to an exponential decay of 0.9 ps (1.5 meV).

sidebands. We then analyze the zero-phonon linewidth for values of τ down to 10 μs , and then to 250 ns.

C. Photon correlation Fourier spectroscopy results

Figure 2 presents the typical variation of $\sqrt{2G_n(t, \tau)}$ as a function of the temporal path difference d_t for a rather long delay τ of 1 ms (the data correspond to NC₁). Large oscillations with a period of 150 fs are observed. They originate from the beats between the ZPL and the two phonon LO replicas [see Fig. 1(a)]. The contrast drops from 1 to 0.3 when increasing the temporal path difference from 0 to 1 ps. This very fast drop of the contrast, i.e., of the optical coherence, has been tentatively attributed to the acoustic phonon pedestal in CdSe/ZnS NCs [20]. However due to the lack of correlation between PCFS method and conventional spectroscopy, this attribution remained unclear. Here, we find that the contrast measured on the consecutive peaks decays with a characteristic time of the order of 0.9 ps, corresponding to a linewidth of 1.5 meV (Fig. 2). This value is in good agreement with the LA phonon pedestal linewidth deduced from the PL spectrum around the ZPL [Fig. 1(b)], that allows us to unambiguously conclude that the very fast drop of the contrast is due to the coupling with LA phonons. This attribution is further confirmed when comparing the relative weight of the ZPL and the LA phonon replica. Indeed we found a very good agreement with the two methods. From the PCFS method, the relative intensity of the ZPL is directly given by the value of the contrast at a temporal path such that LA phonons do not contribute to the signal. We obtain a relative weight of $\sim 30\%$ by taking the value of the contrast at $d_t = 1$ ps. From the PL spectrum, neglecting the LO phonon contribution, we obtain a relative weight of 35% for the ZPL.

The decay of the remaining contrast ($d_t > 1$ ps), i.e., the linewidth of the ZPL, is now investigated for delays τ ranging from 250 ns to 1 ms in order to measure the effect of the SD. First, Fig. 3 displays the decay of the contrast for a short delay τ of 10 μs (for another NC noted NC₂). Starting from about 40%, it indicates that 40% of the emission corresponds to the ZPL, a value close to the one obtained for NC₁. For $d_t > 1$ ps, the curve can be fitted by an exponential decay of time scale $T_2 = 14$ ps, corresponding to a linewidth $\hbar/T_2 = 46$ μeV (or 50 μeV given the experimental uncertainty).

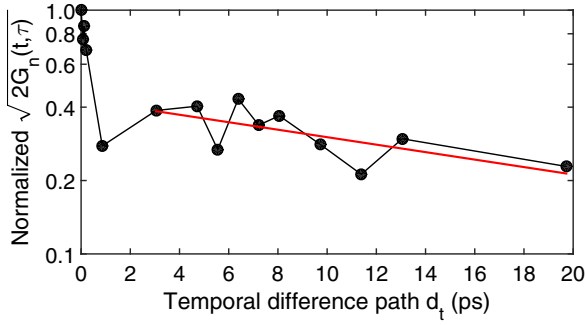


FIG. 3. (Color online) Normalized value of $\sqrt{2G_n(t, \tau)}$ as a function of the temporal difference path for $\tau = 10 \mu\text{s}$ (in semilog scale). The normalization is made with the value of $\sqrt{2G_n(t, \tau)}$ at zero delay. The red line represents a linear fit corresponding to the delays d_t above 3 ps and corresponds to a linewidth of $46 \mu\text{eV}$.

For τ between $10 \mu\text{s}$ and 10ms , there are only little variations of the measured contrast as a function of τ , showing the moderate influence of SD in these time scales (see Fig. 4). For a value of $d_t = 0.12 \text{ps}$ corresponding to a spectral range $\hbar/d_t = 5.5 \text{meV}$, i.e., a temporal delay path close to zero and a high contrast (curve with \bullet), the decay of $\sqrt{2G_n(t, \tau)}$ is negligible. Remarkably, at a temporal difference $d_t > 1 \text{ps}$ such as SD effects are considerably enhanced (the longer the delay d_t , the higher the effect of the SD on the contrast of the fringes), the decay is significant but not drastic (curve with \blacktriangle in Fig. 4 corresponding to $d_t = 13 \text{ps}$ and a narrower spectral range of $\hbar/d_t = 50 \mu\text{eV}$). This weak dependence can be extrapolated to a scale up to 1s with the PL spectrum. Indeed the lower bound of the ZPL linewidth given by the resolution of the spectrometer ($150 \mu\text{eV}$) for NC_1 is fairly similar to those deduced from the PCFS method for the NC_2 . These striking features highlight the weak role played by the SD above $10 \mu\text{s}$ in the ZPL broadening.

However, one could think that a residual contrast could be observed at longer temporal path difference d_t for shorter delays τ . For $\tau < 2 \mu\text{s}$, only the cross correlations \tilde{G}_{ab} and \tilde{G}_{ba} can be used as the autocorrelations are affected by after-pulsing, so that the normalized function G_n cannot be plotted. In order to probe the variations of the ZPL linewidth on a

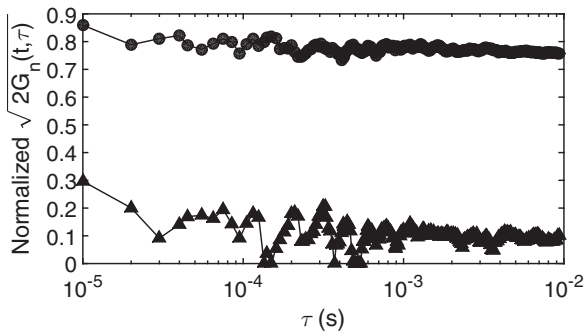


FIG. 4. (a) Normalized value of $\sqrt{2G_n(t, \tau)}$ as a function of the delay τ for $d_t = 0.12 \text{ps}$ (\bullet) and $d_t = 13 \text{ps}$ (\blacktriangle). $\sqrt{2G_n(t, \tau)}$ is normalized to the value of $\sqrt{2G_n(t, \tau)}$ measured at zero delay in Fig. 3.

sub- μs time scale in spite of the APD after-pulsing, we took advantage of the complete suppression of blinking for the CdSe/CdS NCs [7] (it has been demonstrated on these NCs at time scales as short as 50ns through the analysis of the autocorrelation function of the intensity).

This striking property opens opportunities in terms of PCFS measurements when compared to the aforementioned analysis. In the absence of blinking and for a single-state emission showing perfect Poissonian intensity fluctuations, the term $\overline{I(t)I(t+\tau)}$ is independent of τ . We have $\overline{I(t)I(t+\tau)} = \overline{I(t)I(t)} = \overline{I(t)^2}$ so that it is not necessary to calculate $G_n(t, \tau)$ to eliminate the term $\overline{I(t)I(t+\tau)}$. Equation (2) leads to:

$$\frac{\tilde{G}_{ab}(t, \tau)}{\overline{I(t)^2}} = 1 - \mathcal{E}^2(d_t) \hat{p}_\tau(d_t). \quad (5)$$

The difference between the normalized cross correlations $\tilde{G}_{ab}(t, \tau)/\overline{I(t)^2}$ and 1 then provides direct information on the dynamics of the linewidth broadening due to the term $\hat{p}_\tau(d_t)$ (if SD is observed, the normalized cross correlations is lower than 1). In principle, $\mathcal{E}^2(d_t) \hat{p}_\tau(d_t)$ could even be measured by this approach as through $G_n(t, \tau)$ but the low values of the contrast and of the signal to noise ratio in fact prevent its accurate measurement.

Let us consider two long temporal paths ($d_t = 67 \text{ps}$ for NC_1 and $d_t = 46 \text{ps}$ for NC_2 corresponding respectively to spectral ranges $\hbar/d_t = 9.8 \mu\text{eV}$ and $14 \mu\text{eV}$). For these temporal path differences, no contrast is detected at values of τ greater than $10 \mu\text{s}$. Figure 5 shows the variations of the normalized cross correlations with τ ranging between 250ns and 1ms . No variations are detected over four decades. For delays ranging from 250ns to 1ms , $\tilde{G}_{ab}(t, \tau)/\overline{I(t)^2}$ remains close to 1. No SD can be evidenced. At time scales larger than 250ns , SD is then not at the origin of the contrast disappearance for these two long temporal path differences d_t .

D. Discussion

The results presented in the previous section show that the very thick-shell NCs that are always ionized exhibit a ZPL with a linewidth of $50 \mu\text{eV}$. Moreover, above the time scale of 250ns , the effect of SD remains weak. It is noteworthy that the value of $50 \mu\text{eV}$ of the trion recombination linewidth is about one order of magnitude larger than the one measured for the

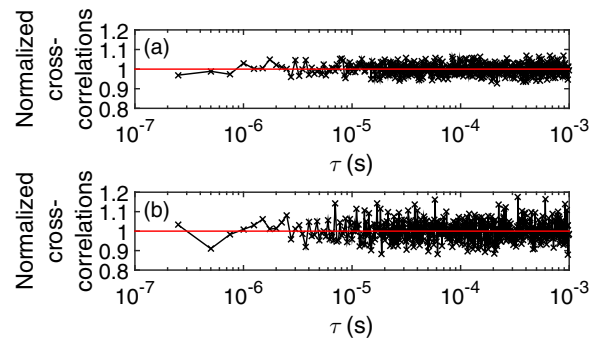


FIG. 5. (Color online) (a) Evolution of $\tilde{G}_{ab}(t, \tau)/\overline{I(t)^2}$ as a function of τ at $d_t = 67 \text{ps}$ for NC_1 . (b) Evolution of $\tilde{G}_{ab}(t, \tau)/\overline{I(t)^2}$ as a function of τ at $d_t = 46 \text{ps}$ for NC_2 .

exciton in standard CdSe/ZnS NCs ($6.5 \mu\text{eV}$, [19]) and three times the one measured for CdSe/CdS NCs with a 5-nm shell ($\sim 15 \mu\text{eV}$ [23]). Such an effect on the linewidth emission at 4 K is specific to colloidal NCs. For InAs/GaAs quantum dots grown by molecular beam epitaxy, no broadening of the charged exciton line with respect to the neutral exciton line is observed [26] (these dots can be inserted in charge-tunable structures and an easy comparison between neutral and charged exciton linewidths can be performed).

However, in InAs/GaAs quantum dots, due to the enhancement of Coulomb interactions generated by the presence of a third charge, the trion can present a larger coupling with an additional source of decoherence, such as a phonon bath, at the origin of linewidth broadening. Urbaszek *et al.* showed that the emission linewidth for InAs/GaAs dots increases with the temperature with a higher rate for the negatively charged trion than for the neutral exciton [26]. The third charge induces a decrease of the emission coherence of the trion state when compared to the exciton state.

In the case of colloidal NCs, it is well known that small charge fluctuations in the surrounding environment of the NC may introduce fast SD at very short time scales [27]. Due to the presence of a third charge, the trion is known to present a larger polarizability than the exciton and is more coupled to the local electrical field fluctuations [28,29]. The results of Figs. 4 and 5 show that this fast phenomenon should occur at time scales τ lower than 250 ns. Depending whether the time scale of the environment fluctuations is longer or shorter than the radiative lifetime, these fast fluctuations may result either in spectral diffusion or decoherence. The fact that, for InAs/GaAs quantum dots, the trion emission is not broadened at 4 K with respect to the neutral exciton emission [26] can be explained by the widely observed tendency that the quantum

dot environment is better controlled, as demonstrated by their absence of blinking and very low spectral diffusion.

IV. CONCLUSION

In conclusion, the trion fluorescence linewidth of very thick-shell CdSe/CdS NCs has been studied in detail by PCFS and standard spectroscopy. At 4 K, the emission of these charged NCs shows no blinking and a high photostability that provides possibilities in terms of PCFS measurements. The time-coherence dynamics is resolved at a time scale as short as 250 ns. The ZPL is characterized by a linewidth broadened at a value of the order of $50 \mu\text{eV}$. This broadening is larger than the one observed for the exciton. We propose that it is explained by the addition of a third charge that weakens the coherence of the excited state through its stronger coupling to the environment. The presented results show that a thick shell can reduce the effect of SD at time scales higher than 250 ns. But they also highlight that preventing the ionization of thick-shell CdSe/CdS NCs is crucial if one wants to use them in the field of quantum information processes based on quantum photon interferences.

ACKNOWLEDGMENTS

The authors thank Paul Voisin and Benoît Eble for fruitful discussions. This work has been supported by the Région Ile-de-France in the framework of the DIM “des atomes froids aux nanosciences”, and the Institut Universitaire de France. B.D., L.B., and J.-P.H. also thank Agence Nationale de la Recherche (Grants No. Core/Shell ANR-08-BLAN-0034 and No. QDOTICS ANR-12-BS10-0008) for funding. L.C. acknowledges funding by Agence Nationale de la Recherche (Grant No. PONIMI ANR-12-JS04-0011).

-
- [1] B. Mahler, P. Spinicelli, S. Buil, X. Quélin, J.-P. Hermier, and B. Dubertret, Towards non-blinking colloidal quantum dots, *Nat. Mat.* **7**, 659 (2008).
 - [2] Y. F. Chen, J. Vela, H. Htoon, J. L. Casson, D. J. Werder, D. A. Bussian, V. I. Klimov, and J. A. Hollingsworth, “Giant” Multishell CdSe nanocrystal quantum dots with suppressed blinking, *J. Am. Chem. Soc.* **130**, 5026 (2008).
 - [3] F. Garcia-Santamara, Y. Chen, J. Vela, R. D. Schaller, J. A. Hollingsworth, and V. I. Klimov, Suppressed Auger recombination in “Giant” nanocrystals Boosts optical gain performance, *Nano Lett.* **9**, 3482 (2009).
 - [4] F. Garcia-Santamaria, S. Brovelli, R. Viswanatha, J. A. Hollingsworth, H. Htoon, S. Crooker, and V. I. Klimov, Break-down of volume scaling in Auger recombination in CdSe/CdS heteronanocrystals: The role of the core–shell interface, *Nano Lett.* **11**, 687 (2011).
 - [5] P. Spinicelli, S. Buil, X. Quélin, B. Mahler, B. Dubertret and J.-P. Hermier, Bright and grey states in CdSe-CdS nanocrystals exhibiting strongly reduced blinking, *Phys. Rev. Lett.* **102**, 136801 (2009).
 - [6] C. Javaux, B. Mahler, B. Dubertret, A. Shabaev, A. V. Rodina, Al. L. Efros, D. R. Yakovlev, F. Liu, M. Bayer, G. Camps, L. Biadala, S. Buil, X. Quélin, and J.-P. Hermier, Thermal activation of non-radiative Auger recombination in charged colloidal nanocrystals, *Nat. Nano* **8**, 206 (2013).
 - [7] D. Canneson, L. Biadala, S. Buil, X. Quélin, C. Javaux, B. Dubertret, and J.-P. Hermier, Blinking suppression and biexcitonic emission in thick-shell CdSe/CdS nanocrystals at cryogenic temperature, *Phys. Rev. B* **89**, 035303 (2014).
 - [8] M. Nirmal, B. O. Dabbousi, M. G. Bawendi, J. J. Macklin, J. K. Trautman, T. D. Harris, and L. E. Brus, Fluorescence intermittency in single cadmium selenide nanocrystals, *Nature (London)* **383**, 802 (1996).
 - [9] S. A. Empedocles, D. J. Norris, and M. G. Bawendi, Photoluminescence spectroscopy of single CdSe nanocrystallite quantum dots, *Phys. Rev. Lett.* **77**, 3873 (1996).
 - [10] R. G. Neuhauser, K. T. Shimizu, W. K. Woo, S. A. Empedocles, and M. G. Bawendi, Correlation between fluorescence intermittency and spectral diffusion in single semiconductor quantum dots, *Phys. Rev. Lett.* **85**, 3301 (2000).
 - [11] M. J. Fernée, B. Littleton, T. Plakhotnik, H. Rubinsztein-Dunlop, D. E. Gómez, and P. Mulvaney, Charge hopping revealed by jitter correlations in the photoluminescence spectra of single CdSe nanocrystals, *Phys. Rev. B* **81**, 155307 (2010).

- [12] T. Plakhotnik, M. J. Fernée, B. Littleton, Halina Rubinsztein-Dunlop, C. Potzner, and Paul Mulvaney, Anomalous power laws of spectral diffusion in quantum dots: A connection to luminescence intermittency, *Phys. Rev. Lett.* **105**, 167402 (2010).
- [13] M. J. Fernée, T. Plakhotnik, Y. Louyer, B. N. Littleton, C. Potzner, P. Tamarat, P. Mulvaney, and B. Lounis, Spontaneous spectral diffusion in CdSe quantum dots, *Phys. Chem. Lett.* **3**, 1716 (2012).
- [14] M. Saba, M. Aresti, F. Quochi, M. Marceddu, M.-A. Loi, J. Huang, D. V. Talapin, A. Mura, and G. Bongiovanni, Light-induced charged and trap states in colloidal nanocrystals detected by variable pulse rate photoluminescence spectroscopy, *ACS Nano* **7**, 229 (2013).
- [15] T. Plakhotnik and Daniel Walser, Time resolved single molecule spectroscopy, *Phys. Rev. Lett.* **80**, 4064 (1998).
- [16] G. Sallen, A. Tribu, T. Aichele, R. André, L. Besombes, C. Bougerol, M. Richard, S. Tatarenko, K. Kheng, and J. Ph. Poizat, Subnanosecond spectral diffusion measurement using photon correlation, *Nat. Photon.* **4**, 696 (2010).
- [17] X. Brokmann, M. Bawendi, L. Coolen, and J.-P. Hermier, Photon-correlation Fourier spectroscopy, *Opt. Expr.* **14**, 6333 (2006).
- [18] L. Coolen, X. Brokmann, and J.-P. Hermier, Modeling coherence measurements on a spectrally diffusing single-photon emitter, *Phys. Rev. A* **76**, 033824 (2007).
- [19] L. Coolen, X. Brokmann, P. Spinicelli, and J.-P. Hermier, Emission characterization of a single CdSe-ZnS nanocrystal with high temporal and spectral resolution by photon-correlation fourier spectroscopy, *Phys. Rev. Lett.* **100**, 027403 (2008).
- [20] L. Coolen, P. Spinicelli, and J.-P. Hermier, Emission spectrum and spectral diffusion of a single CdSe/ZnS nanocrystal measured by photon-correlation Fourier spectroscopy, *J. Opt. Soc. Am. B* **26**, 1463 (2009).
- [21] J. Wolters, N. Sadzak, A. W. Schell, T. Schröder, and O. Benson, Measurement of the ultrafast spectral diffusion of the optical transition of nitrogen vacancy centers in nano-size diamond using correlation interferometry, *Phys. Rev. Lett.* **110**, 027401 (2013).
- [22] L. F. Marshall, J. Cui, X. Brokmann, and Mounji G. Bawendi, Extracting spectral dynamics from single chromophores in solution, *Phys. Rev. Lett.* **105**, 053005 (2010).
- [23] A. P. Beyler, L. F. Marshall, J. Cui, X. Brokmann, and Mounji G. Bawendi, Direct observation of rapid discrete spectral dynamics in single colloidal CdSe-CdS core-shell quantum dots, *Phys. Rev. Lett.* **111**, 177401 (2013).
- [24] D. Canneson, I. Mallek-Zouari, S. Buil, X. Quélin, C. Javaux, B. Dubertret, and J.-P. Hermier, Enhancing the fluorescence of individual thick shell CdSe/CdS nanocrystals by coupling to gold structures, *New J. Phys.* **14**, 063035 (2012).
- [25] S. Brovelli, R. D. Schaller, S. A. Crooker, F. García-Santamaría, Y. Chen, R. Viswanatha, J. A. Hollingsworth, H. Htoon, and V. I. Klimov, Nano-engineered electron-hole exchange interaction controls exciton dynamics in core-shell semiconductor nanocrystals, *Nat. Commun.* **2**, 280 (2011).
- [26] B. Urbaszek, E. J. McGhee, M. Krüger, R. J. Warburton, K. Karrai, T. Amand, B. D. Gerardot, P. M. Petroff, and J. M. Garcia, Temperature-dependent linewidth of charged excitons in semiconductor quantum dots: Strongly broadened ground state transitions due to acoustic phonon scattering, *Phys. Rev. B* **69**, 035304 (2004).
- [27] M. J. Fernée, C. Sinito, Y. Louyer, C. Potzner, T.-L. Nguyen, P. Mulvaney, P. Tamarat, and B. Lounis, Magneto-optical properties of trions in non-blinking charged nanocrystals reveal an acoustic phonon bottleneck, *Nat. Commun.* **3**, 1287 (2012).
- [28] K. Kowalik, O. Krebs, P. Senellart, A. Lemaître, B. Eble, A. Kudelski, J. Gaj, and P. Voisin, Stark spectroscopy of coulomb interactions in individual InAs/GaAs self-assembled quantum dots, *Phys. Stat. Sol. (c)* **3**, 3890 (2006).
- [29] P. Michler, *Single Quantum Dots: Fundamentals, Applications and New Concepts* (Springer, Berlin, 2003).